Full length article

# Minor additions of Sn suppress the omega phase formation in beta titanium alloys

Florian Brumbauer [a],[*], Norihiko L. Okamoto [b], Tetsu Ichitsubo [b], Wolfgang Sprengel [a], Martin Luckabauer [c],[*]

[a] Institute of Materials Physics, NAWI Graz, Graz University of Technology, Petersgasse 16, 8010, Graz, Austria
[b] Institute for Materials Research, Tohoku University, 2-1-1 Katahira Aoba-ku, Miyagi 980-8577, Sendai, Japan
[c] Faculty of Engineering Technology, University of Twente, De Horst 2, 7522LW, Enschede, The Netherlands

ARTICLE INFO

ABSTRACT

A critical characteristic of $\beta$-Ti alloys is the inevitable formation of $\omega$-precipitates during certain heat treatments which leads to embrittlement, or even to a complete loss of ductility. Therefore, alloy design with the goal to inhibit the elementary $\omega$-formation process is of utmost importance. Here, we propose a design strategy for prototypical $\beta$-type Ti–Cr–(Mo) alloys to alleviate this problem using only minor additions of Sn. Upon addition of Sn, we observed an extensive deceleration or even suppression of the $\omega$-formation kinetics during isothermal ageing. Furthermore, the internal friction response of the elementary formation process indicated a decisive reduction of potential $\omega$-nucleation sites, while the activation energy of the process remained almost unchanged. The results show, that the addition of Sn can significantly increase the width of the time–temperature process window and the long-time ageing resistance of $\beta$-Ti alloys, opening up huge opportunities for advanced alloy design and manufacturing routes.

## 1. Introduction

$\beta$-Ti alloys offer a huge innovative potential by taking advantage of their complex microstructures attainable that permit tailoring mechanical as well as functional properties to the applications demands. Apart from their exceptional fatigue resistance [1], biocompatibility and excellent corrosion resistance [2], their unusually large range of elastic properties (E $\approx$ 40 to 100 GPa [3]) makes them very promising candidates for low-modulus biomedical implants by preventing stress-shielding of the bone and thereby promoting bone remodelling [4]. Despite their seemingly outstanding properties, they suffer a severe problem: the inevitable formation of metastable $\omega$-phase strongly deteriorates their mechanical properties leading to embrittlement or often to a complete loss of ductility. [5,6] The transition metals Ti, Zr and Hf exhibit a peculiar elastic anomaly in their high-temperature bcc modification, where the longitudinal phonon with $q = \frac{2}{3}[111]$ seemingly vanishes. [7–9] In alloys where the $\beta$-phase is stabilised, this fundamental property allows neighbouring $[111]_\beta$-planes to collapse onto each other by the alignment of linear displacement defects in the $\langle 111 \rangle$ direction resulting in a hexagonal structure, i.e., the $\omega$-phase. [10–12] Despite this elementary formation process, three different formation mechanisms for the $\omega$-phase are differentiated related to their

athermal transformation temperature $T_{ath}$, which is thought to be a limiting region of stability for the $\beta$-modification [13]: (i) the athermal $\omega_{ath}$-phase, which forms during quenching from above the $\beta$-transus temperature upon undershooting $T_{ath}$, (ii) the diffusion-assisted $\omega_{iso}$-phase, which forms during isothermal ageing notably above $T_{ath}$ where the decomposition in $\beta$-stabiliser depleted and $\beta$-stabiliser enriched regions driven by diffusion leads to a destabilisation of the $\beta$-phase and (iii) diffusion-less isothermal $\omega_{dl,iso}$, where quenched-in regions depleted in $\beta$-stabiliser content around $T_{ath}$ locally transform without preceding diffusion (see Fig. 1). [14,15]

The mentioned phenomena motivate research with the goal to inhibit or slow down the elementary $\omega$-formation process by appropriate alloy design. To find a suitable alloy system that inhibits the elementary process, one needs to find possible candidate elements that fulfil several requirements: (i) do not stabilise the $\alpha$-phase, (ii) are readily available, (iii) show high affinity to Ti, i.e., solubility in the $\beta$-phase, (iv) are ideally not an interstitial to keep the superior ductility and (v) are biocompatible. Sn seems to be an ideal choice since it is neutral to both $\alpha$ and $\beta$ phases [2,15], has an adequate solubility and is considered a non-toxic element [16]. Most importantly, there

---

* Corresponding author.
E-mail addresses: f.brumbauer@tugraz.at (F. Brumbauer), nlokamoto@tohoku.ac.jp (N.L. Okamoto), tichi@imr.tohoku.ac.jp (T. Ichitsubo), w.sprengel@tugraz.at (W. Sprengel), m.luckabauer@utwente.nl (M. Luckabauer).
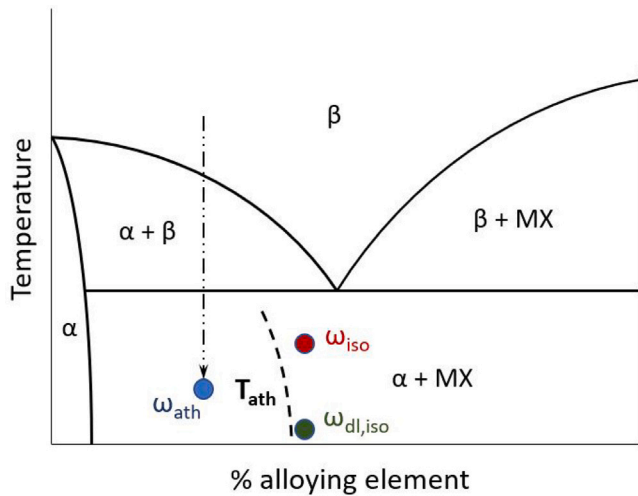
**Fig. 1.** Schematic phase diagram for $\beta$-eutectoid titanium alloy systems adapted from Ref. [6]. The dashed curve represents the lower limit of stabiliser content where the $\beta$-phase is retained after quenching (dash-dotted line), termed $T_{ath}$. The phases $\omega_{ath}$ (blue), $\omega_{dl,iso}$ (green) and $\omega_{iso}$ (red) denote the three different mechanisms of $\omega$-phase formation. Furthermore, MX denotes intermetallic compounds found in this type of equilibrium phase diagrams. (For interpretation of the references to colour in this figure legend, the reader is referred to the web version of this article.)

is evidence that additions of Sn increase the stability of the $\beta$-phase and substantially reduce the volume fraction of $\omega$-phase formed.[17–19] Therefore, this study aims to evaluate the effect of Sn addition on the $\omega$-precipitation kinetics of prototypical $\beta$-Ti alloys and subsequently reveal its underlying influence on the elementary formation process.

## 2. Experimental

We prepared sample ingots with a nominal composition of Ti-12Cr, Ti–12Cr–1Sn and Ti–12Cr–3Sn (at.%) from high-purity Ti (purity: $\geq$ 99.999 by wt.%, O < 300 ppm), Cr (purity: 99.9 by wt.%) and Sn (purity: 99.99 by wt.%) by arc melting in a Zr-gettered Ar-atmosphere at a pressure of $\sim$500 mbar. To ensure homogeneity, these ingots were remelted multiple times. For the measurements at cryogenic temperatures, 4 at.% of Cr were substituted for the same relative amount of Mo to reliably prevent $\omega_{ath}$-formation down to temperatures below the $\omega_{ath}$-transition temperature observed by Luhman et al. [20]. Furthermore, Mo is thought to sufficiently enhance the stability of the $\beta$-phase without facing a potentially accelerated formation of intermetallic phase at grain boundaries when increasing the Cr-content above the eutectoid concentration in the alloy. Therefore, pure Mo (purity: 99.95 by wt.%) was melted into the already homogenised TiCr(Sn) primary ingots resulting in nominal compositions of Ti–4Mo–8Cr, Ti–4Mo–8Cr–1Sn, Ti–4Mo–8Cr–2Sn, Ti–4Mo–8Cr–3Sn and Ti–4Mo–8Cr–4Sn (at.%). This procedure of alloying into the already homogenised primary ingots assures a homogeneous distribution of the refractory metal. For future applications and fabrication processes, e.g. medical implants made by additive manufacturing, the addition of Mo is not expected to have significant advantages and consequently the precipitation kinetics were studied for the alloys containing only Cr and Sn. After production, the alloys were either Cu-mold gravity cast into rod shaped samples with a diameter of $\sim$6 mm, or directly cold-rolled for rectangular-shaped samples depending on the experimental method used. Furthermore, all samples were homogenised at 1000 °C in evacuated and fused silica ampules for $\sim$24 h before quenching in iced water. To achieve microstructures suitable for powder diffraction, the homogenised blocks were cold-rolled in different directions up to around 50% of deformation and subsequently recrystallised in the two-phase region at 620 °C for 30 min followed by $\beta$-annealing at 750 °C for 45 min.

For the differential scanning calorimetry (DSC) measurements, button shaped samples with a mass of $\sim$25 mg were machined from the cast Ti12Cr and Ti12Cr3Sn alloys. We determined the heat-flux using a Netsch Pegasus 404 at heating/cooling rates of 10 K min$^{-1}$. High purity (5N) Argon was used as purge gas with an additional Zr-getter in the vicinity of the alumina sample pans.

For the dilatometric measurements, cylindrical samples were machined from the cold-rolled Ti12Cr, Ti12Cr1Sn and Ti12Cr3Sn alloys with an initial length of $\sim$12 mm and a diameter of 4.7 mm. We recorded the relative length change $\Delta L/L_0$ after in-situ quenching from the $\beta$-phase region at various isothermal ageing temperatures between 190 °C and 370 °C under high vacuum conditions using the high-stability laser dilatometer described in detail elsewhere. [21] To this end, the samples were solution treated at 800 °C for at least 30 min following the procedure described by Enzinger et al. [14] Subsequently, the Ti12Cr and the Ti12Cr1Sn alloys were directly quenched to their respective ageing temperature using a high purity (5N) He-gas stream at a quenching rate of $\sim$20 to 25 K s$^{-1}$. For the Ti12Cr3Sn alloy, we chose a modified indirect approach where the sample was quenched to 30 °C for $\sim$4 min before re-heating to the respective ageing temperature with 100 to 120 K min$^{-1}$. This modification ensured the highest accuracy of the expected small effect on the length change after quenching at the expense of minor loss of the early precipitation behaviour. Furthermore, the dilatometer was, for the direct as well as for the indirect-quenching approach, constantly flushed with a high purity (5N) Ar-gas stream of 20 to 40 standard cubic centimetres per minute to support the PID control unit regarding a fast responsiveness after He-quenching and high long-time stability during ageing. This constant Ar-flow resulted in a vacuum chamber pressure of $8.5 \times 10^{-3}$ mbar. Reproducibility and device-related uncertainties of the measurements as well as irreversible changes inside the samples were excluded by validating the dilatometric measurement at 310 °C with preceding measurements as well as reference samples (Ta, purity >99.95 wt.%).

For the electromagnetic acoustic resonance (EMAR) measurements, cylindrical samples were machined from the cast TiMoCr(Sn) alloys with an initial length of $\sim$7 mm and a diameter of 4 mm. We observed the change in resonance frequency using a self-developed, contactless spectrometer based on a Nb$_3$Sn superconducting magnet similar to the principle setup described by Ogi et al. [22] with a device-related uncertainty of 2 Hz in the excitation range of 1 MHz. The temperature of the sample holder was controlled by a closed cycle He-cryostat. Furthermore, the magnetic field strength was kept constant for all experiments at 1.5 T. The damping coefficient $\alpha_M$ of the acoustic wave was determined according to the free-decay method [23] by fitting an exponential decay function to the decay of the same acoustic resonance mode for all samples. The mode frequency at room temperature was found at $f_R \simeq 850$ kHz. Thereafter, we measured the change in resonance frequency $f_R$ and the damping coefficient $\alpha_M$ of the same mode at intervals of $\sim$1 K during continuous cooling of the sample from 300 K down to $\sim$4 K. From the observed change in $f_R$ and $\alpha_M$ the internal friction $Q^{-1}$ was determined according to

$$Q^{-1} = \frac{\alpha_M}{\pi\,f_R}. \tag{1}$$

For the X-ray diffraction (XRD) measurements, the rectangular-shaped TiCr(Sn) samples were ground with SiC-paper, polished with diamond suspensions and finished with colloidal silica for a deformation-free surface. Complementing the dilatometric measurements, we recorded XRD patterns between 67 and 90° during isothermal ageing at 250 °C using a Bruker D8 Discover X-ray diffractometer with Cu-K$_{\alpha_{1,2}}$ radiation and an illuminated area of $\sim$10 × 4 mm in Bragg-Bretano geometry. A LYNXEYE XE-T 2D high energy resolution (<380 eV) detector was used for data acquisition. Furthermore, the sample temperature was controlled using a Linkam THMS600 heating/cooling stage. In contrast to the dilatometric measurements, these patterns were recorded ex-situ, i.e., the samples were cyclically heated with 150 K min$^{-1}$, held

at 250 °C followed by controlled cooling with gaseous $N_2$ at a quenching rate of ~150 K min$^{-1}$ to 30 °C before performing long-exposure measurements. The position of the $(211)_\beta$-peak and consequently the lattice parameter of the $\beta$-phase were evaluated by fitting the XRD-peaks using a Lorentzian function with a resulting uncertainty of ~6 × 10$^{-4}$ Å. Complementing the EMAR measurements, we recorded XRD patterns between 50 and 90° at ambient as well as at cryogenic temperatures of 160 K and 100 K using the same setup.

## 3. Results

### 3.1. Enhanced stability of $\beta$-phase by addition of Sn

The unique combination of properties ascribed to $\beta$-Ti alloys is rooted in the complex microstructures achievable by numerous heat treatment possibilities. Therefore, their temperature dependent transformation behaviour is of utmost interest. We determined the precipitation sequence and their transformation temperatures for the Ti12Cr and Ti12Cr3Sn alloys using DSC (see Fig. 2) and assigned the respective peaks following previous studies from Okamoto et al. [13] and Bönisch et al. [24]. We observed two peaks at around 300 and 350 °C for the Ti12Cr alloy ascribed to the formation of $\omega_{iso}$-precipitates. For the Ti12Cr3Sn alloy, a single $\omega_{iso}$-formation peak slowly rises around 250 °C. Not only is the peak shifted by ~100 °C but most importantly the absolute quantity of exothermic heat is vanishingly small compared to the alloy without Sn. With further heating, the formed $\omega$-precipitates partially dissolve in the Ti12Cr alloy at around 400 °C and/or transform to $\alpha$-phase at favourable sites (denoted as $\alpha_P$ in Fig. 2), e.g. at grain boundaries. Above around 550 °C, $\alpha$-precipitation inside grains sets in before gradually dissolving when approaching the $\beta$-transus temperature at around 700 °C. For the Ti12Cr3Sn alloy, the formed $\omega_{iso}$-precipitates dissolve at around 300 °C. Subsequently, hardly any change in phase composition is observed below 550 °C. Above 550 °C, $\alpha$-precipitation gradually sets in again with a strongly reduced absolute quantity of exothermic heat. At around 720 °C, the $\alpha$-precipitates dissolve. During cooling from above 850 °C, we observed an extensive peak at around 320 °C associated with the formation of $\omega_{iso}$-precipitates in the Ti12Cr alloy. Interestingly, in contrast to the Ti12Cr alloy the Ti12Cr3Sn alloy shows neither a peak associated with $\omega_{iso}$-precipitation nor with $\alpha$-transformation, solely the natural change of heat capacity with temperature is observed. Therefore, the $\beta$-phase seems to be strongly stabilised by the addition of 3 at.% Sn. This distinct difference in transformation behaviour during cooling is supported by hardness measurements. The strong $\omega_{iso}$-formation peak found in the Ti12Cr alloy led to an increase in hardness after cooling of 174 HV1 compared to its as-quenched condition with an initial hardness of (290 ± 5) HV1. The addition of 3 at.% Sn for the Ti12Cr3Sn alloy hardly changed the hardness after cooling with a reduction of 10 HV1 (initial hardness after quench: (295 ± 5) HV1). These results unambiguously show a retarded transformation kinetics evoked by the addition of Sn to the alloy and the detrimental effect of $\omega$-phase precipitation on the mechanical properties. The observed strong stabilisation effect of the $\beta$-phase whilst still preserving the low elastic modulus of the alloy is supported by first-principle calculations. [25] The consequences of this transformation behaviour on the precipitation kinetics of the $\omega_{iso}$-phase will be evaluated in the following sections.

### 3.2. Strongly decelerated precipitation kinetics of $\omega_{iso}$-phase

The diffusion-assisted isothermal formation of $\omega_{iso}$-phase at temperatures considerably above $T_{ath}$ (found at ~10 at.% Cr at ambient temperature after quenching [26–30]) is preceded by a decomposition process into Cr-lean regions embedded in a surrounding Cr-rich matrix. Whilst still remaining the $\beta$-phase, the change in Cr-content manifests itself in a local swelling of the Cr-depleted regions and a contraction of the surrounding Cr-enriched matrix. Both effects arise from the
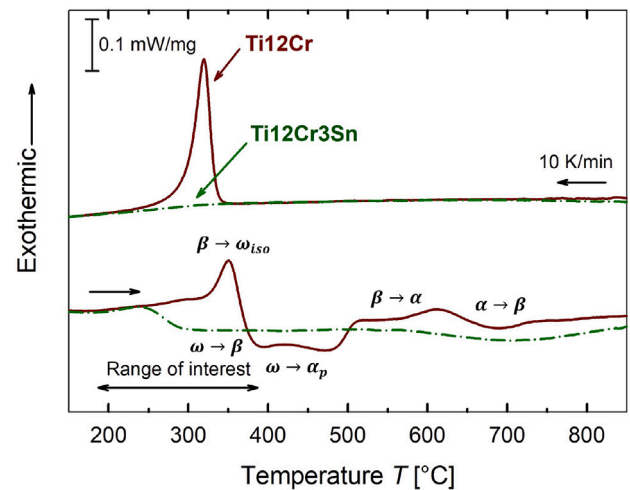


**Fig. 2.** DSC profiles measured for the Ti12Cr alloy (red) and Ti12Cr3Sn alloy (green, dash dotted) at a cooling/heating rate of 10 K min$^{-1}$. For the Ti12Cr alloy an intense $\omega$-formation peak occurs around 320 °C, which is not observed for the Ti12Cr3Sn alloy.

linearly decreasing lattice constant with increasing Cr-content in the alloy. [14,26] With progressing decomposition, the Cr-content locally approaches concentrations below $T_{ath}$. In those Cr-lean regions the $\beta$-phase becomes increasingly unstable and might act as nucleation sites for $\omega_{iso}$-phase formation. The ongoing decomposition of the alloy continuously provides local regions of depleted $\beta$-stabiliser content where $\omega_{iso}$-phase can be formed. During growth of the $\omega_{iso}$-phase particles, Cr further diffuses into the surrounding matrix whereby the size of the $\omega_{iso}$-phase particles remains within a few nanometres.

To determine the effect of Sn addition on the $\omega_{iso}$-phase formation, we recorded ex-situ XRD patterns after various ageing times at 250 °C (See Fig. 3). For the Ti12Cr alloy, the broad, exposed $(11\bar{2}2)_\omega$-peak appears from its as-quenched condition (Fig. 3(b)). With ongoing ageing time the peak sharpens associated with the growth of more equally sized $\omega$-particles. Furthermore, we observed a shift of the $(211)_\beta$-peak associated with the Cr-enrichment of the $\beta$-Ti matrix (Fig. 3(a)). With the addition of 3 at.% Sn the $(11\bar{2}2)_\omega$-peak is less intense and substantially broader than for the Ti12Cr alloy (Fig. 3(d)). Furthermore, the shift of the $(211)_\beta$-peak is strongly reduced (Fig. 3(c)). Both aspects suggest a smaller fraction of $\omega_{iso}$ particles formed, which tend to remain small in size for comparable ageing times for both alloys. Moreover, the decomposition of the $\beta$-phase in Cr-enriched and Cr-depleted regions seems to be effectively suppressed. Additionally, we observed a significant increase in hardness of 130 HV1 after 48 h for the Ti12Cr alloy (initial hardness after quench: (303 ± 5) HV1), whereas for the Ti12Cr3Sn alloy the hardness hardly changed with 8 HV1 (initial hardness after quench: (295 ± 5) HV1).

For an in-depth assessment of the effect of Sn addition on the precipitation kinetics of $\omega_{iso}$-phase, we recorded the relative length change $\Delta L/L_0$ during isothermal ageing of the Ti12Cr alloys with different Sn content by high-precision laser dilatometry (see Fig. 4). In accordance with Enzinger et al. [14], we observed an initial plateau region followed by a pronounced negative relative length change, i.e. shrinkage, associated with the decomposition and subsequent dominating $\omega_{iso}$-phase formation for the Ti12Cr alloy. The absolute value as well as the nucleation rate increase with increasing isothermal ageing temperature. In the later stages of the transformation, the change in morphology of the $\omega_{iso}$-phase particles from ellipsoidal to cuboidal shape due to the high-strain misfit at the $\beta/\omega_{iso}$-interface might be visible in form of a flattening of the characteristic S-shape during growth of the particles found for transformation processes below 310 °C. [31,32] Above 310 °C, a positive relative length change, i.e. expansion, is superimposed in the
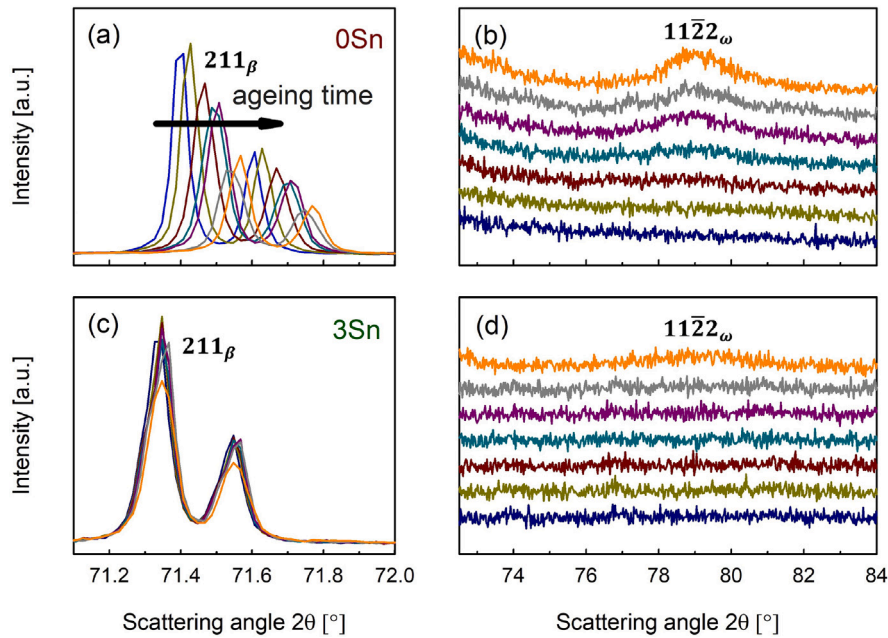
**Fig. 3.** Ex-situ XRD patterns for the (a-b) Ti12Cr alloy and (c-d) for the Ti12Cr3Sn alloy upon isothermal ageing at 250 °C for various times (from bottom to top, as-quenched: blue, 100 s: yellow, 500 s: red, 1000 s: cyan, 5000 s: margenta, 10 000 s: grey, 180 000 s: orange). Compared to the as-quenched condition, the (a) $(211)_\beta$-peak distinctly shifts with progressing ageing for the Ti12Cr alloy accompanied by the occurrence of the distinct (b) $(11\bar{2}2)_\omega$-peak. After the addition of Sn, the (d) $(11\bar{2}2)_\omega$-peak is less intense and substantially broader, which is reflected in a hardly changing (c) surrounding $\beta$-matrix. (For interpretation of the references to colour in this figure legend, the reader is referred to the web version of this article.)

later stages of the transformation, which is associated with the $\omega_{iso} \to \alpha$ transformation. [14]

The addition of as few as 1 at.% Sn revealed a significant shift of the onset time of the negative relative length change, i.e., shrinkage associated with $\omega_{iso}$-phase formation by more than one order of magnitude to prolonged ageing times. This retardation indicates a decisive deceleration of the precipitation kinetics of the $\omega_{iso}$-phase in the Ti12Cr1Sn alloy. Furthermore, the $\omega_{iso} \to \alpha$ transformation seemingly shifts to higher temperatures above 370 °C. For the Ti12Cr3Sn alloy with 3 at.% Sn we did not only observe a proceeding deceleration of the $\omega_{iso}$-phase formation, but an almost complete suppression of shrinkage at all measurement temperatures. Interestingly, when comparing the relative length change with the change in the lattice constant determined from the shift of the $(211)_\beta$-peak, it seems that the occurring contraction is mainly evoked by the Cr-enriching matrix (see. Fig. 4(b)).

Taken together, these results show that already minor additions of Sn can significantly affect, i.e., retard the $\omega_{iso}$-phase formation kinetics in those prototypical $\beta$-Titanium alloys.

*3.3. Diminishing collapse regions of the elementary $\omega$-phase formation process*

Having determined the effect of Sn on the kinetics of $\omega_{iso}$-phase formation, the influence of the Sn addition on the elementary process of the $\omega$-transformation needs to be assessed. Tane et al. [33] suggested, that the elementary process of $\omega$-transformation is associated with a local dynamic collapse of $[111]_\beta$-planes that does not necessarily result in the formation of stable $\omega$-nuclei. Furthermore, Sommer et al. [34,35] related this elementary formation process to an anelastic relaxation as observed by mechanical spectroscopy causing a change in the internal friction response signal, usually referred to as $\Delta M$-effect [36], during the excitation of this local dynamic collapse of planes. We analysed the change in resonance frequency $f_R/f_R^{max}$ and internal friction $Q^{-1}$ in Ti4Mo8Cr alloys with different Sn content using EMAR. EMAR is sensitive to local prone regions, where the dynamic collapse of $[111]_\beta$-planes might lead to the formation of $\omega$-nuclei. These prone regions represent the initial nucleation sites for $\omega_{iso}$-phase precipitation during

isothermal ageing at elevated temperatures. The analysis revealed a steep increase of $f_R/f_R^{max}$ below 200 K, which decisively decreases with increasing Sn addition (see Fig. 5(a)). This increase in $f_R$ is attributed to the change in the elastic modulus by anelastic relaxations related to the broad $Q^{-1}$-peak at ~150 K to 170 K appearing for all alloys. In accordance with Tane et al. [33], this broad peak in the internal friction is associated with a local excitation of the dynamic collapse of $[111]_\beta$-planes, which is in resonance with the induced vibration frequency at the respective temperature. For the validity of the interpretation, it is important to exclude structural changes in the alloys. Therefore, we performed ex-situ XRD at ambient temperature as well as cryogenic temperatures for the Ti4Mo8Cr and Ti4Mo8Cr3Sn alloys (see insets of Fig. 5). For both alloys, we observed no structural changes leading to the conclusion that no $\omega_{ath}$-formation occurs that might be responsible for the change in internal friction response. This suppression of $\omega_{ath}$-formation upon addition of Sn is further reported by Ozaki et al. [37], Hanada et al. [38,39] as well as Matsumoto et al. [40]. Since the dynamic collapse of $[111]_\beta$-planes occurs solely in local regions where the $\beta$-stabiliser content is depleted destabilising the $\beta$-phase, its energy barrier mainly originates from the free energy barrier between $\beta$ and $\omega$ structures and their interface energy in the transition state. [33] To determine the activation energy of the elementary process dependent on the Sn content, we expanded the Debye-oscillator model based on Tane et al. [33] to analyse the temperature dependent internal friction $Q^{-1}(T)$. The local character of the dynamic plane collapse emphasises the necessity to take its spatial dependence into consideration, i.e., $\beta$-stabiliser and Sn content in the surrounding matrix. Therefore, we attributed the elementary process an energy distribution $P(E)$ in form of a Gaussian distribution assuming a similar distribution of $\beta$-stabiliser content in local regions as found by Tane et al. [33] and Choudhuri et al. [41] using atom probe tomography. Those compositional fluctuations and, consequently, their varying degree of $\beta$-phase stabilisation are thought to result in a spatial dependence of the activation energy. The modified Debye-oscillator model can then be written as

$$Q^{-1} = \Delta \int_0^\infty P(E) \frac{\omega_r \tau}{1 + \omega_r^2 \tau^2} \, dE \qquad (2)$$
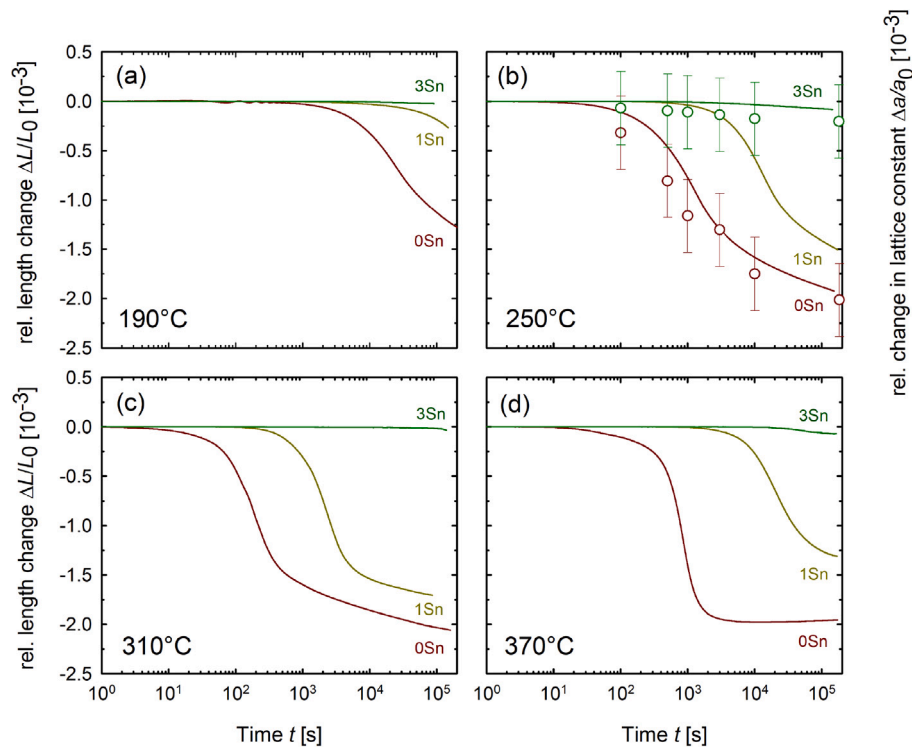
**Fig. 4.** Effect of Sn addition (1 at.% yellow, 3 at.% green) on relative length change $\Delta L/L_0$ for Ti12Cr alloy (red) upon isothermal ageing at (a) 190 °C, (b) 250 °C, (c) 310 °C and (d) 370 °C. Furthermore, in (b) the relative change in lattice constant $\Delta a/a_0$ of the $\beta$-phase determined from the shift of the $(211)_\beta$-peak (see Fig. 3(a) and (c)) is shown for the Ti12Cr and Ti12Cr3Sn alloys (circles). With the addition of Sn, a shift of the onset of $\omega$-phase formation as well as a strong suppression of the extend of volume change is observed. (For interpretation of the references to colour in this figure legend, the reader is referred to the web version of this article.)

with

$$\tau = \tau_0 \exp\left(\frac{E}{k_B T}\right) \tag{3}$$

and the Gaussian activation energy distribution

$$P(E) = \frac{1}{\sqrt{2\pi\sigma^2}} \exp\left(-\frac{1}{2}\left(\frac{E-\mu}{\sigma}\right)^2\right) \tag{4}$$

where $\Delta$ is the relaxation strength, $\omega_r = 2\pi f_R$ is the angular frequency, $\tau_0 = \frac{1}{f_0}$ is the time constant and $k_B$ is the Boltzmann constant. Furthermore, for modelling we neglected quantum-mechanical phenomena and individual excitations with small activation energies at low-temperatures around 50 K and below. The numerical fits of Eq. (2) to the internal friction $Q^{-1}$ (see Fig. 5(b)) revealed a widely distributed activation energy for the elementary process in the range of ~0.05 to 0.30 eV (see Fig. 6(a)) with no significant shift of the mean activation energy $\mu$ at ~0.20 eV caused by the addition of Sn (see Fig. 6(a) and inset of Fig. 6(b)). Furthermore, the relaxation strength $\Delta$ linearly decreases with increasing Sn content in the alloys (see Fig. 6(b)). The uncertainty of the relaxation strength $\Delta$ was estimated by the scattering of the internal friction $Q^{-1}$-peak. Taken together, these results impressively demonstrate that the addition of Sn has indeed no influence on the activation energy of the dynamic collapse of $[111]_\beta$-planes, but actively reduces the number of local collapse regions that might form stable $\omega$-nuclei. The diminishing local collapse regions are reflected in the strongly decelerated or even suppressed precipitation kinetics during isothermal ageing at elevated temperatures when Sn is added to the $\beta$-Ti alloys (see Sections 3.1 and 3.2.).

## 4. Discussion

The elementary process of $\omega$-phase formation is associated with a collapse of a pair of $(111)_\beta$ planes onto a single plane. [5,6] A key prerequisite of this collapse is the alignment of linear displacement

defects consisting of vacancies and crowdions in the $\langle 111 \rangle$ direction, which results in the formation of the characteristic trigonal bonding of the displaced atom in the plane of capture. [10–12] As postulated by Williams et al. [11], solute atoms and their respective stress fields are expected to interact with those linear defects thereby impeding their alignment needed for the $\omega$-phase formation. Therefore, special focus must lie on the interaction of the added Sn with those linear defects. Hu et al. [42] as well as Zhang et al. [43] reported a considerable positive binding energy for Sn-vacancy complexes meaning that Sn solutes are attractive to present vacancies in $\alpha$-Ti similar to those found for Al-based alloys. [44] Further studies proposed a mechanism, where excess vacancies are trapped at Sn solutes thereby controlling the diffusional process and effectively suppressing their precipitation kinetics in Al-based alloys during natural ageing. [45,46] This retardation mechanism is reported to be strongly dependent on the solubility of Sn in those alloys, i.e., increasing solubility of Sn shifts the onset of hardening to longer ageing times. At elevated temperatures during artificial ageing, trapped vacancies are thought to be released from their traps accelerating the formation of precipitates. Čížek et al. [47] further suggested, that clustering of Sn surrounding vacancies cannot be excluded during quenching as well as during ageing at low temperatures. Furthermore, at elevated temperatures thermal vacancies might form Sn-vacancy complexes. Despite the obvious differences between both light metal alloy systems, the effect of Sn addition on the ageing response seems to have strong similarities to the behaviour of Sn in $\beta$-Ti alloys. Therefore, we propose a combined mechanism inspired by the aforementioned interaction of Sn with the alignment of linear displacement defects and their trapping effect on vacancies for the suppressed precipitation kinetics in the studied alloys evoked by the addition of Sn.

We suggest, that a fraction of Sn solutes effectively trap vacancies due to their attractive binding energies thereby reducing the amount of free vacancies. This reduced amount of vacancies retards the local decomposition into Cr-lean and Cr-rich regions necessary for the $\omega_{iso}$-formation by hampering the diffusion process. Such a retarded
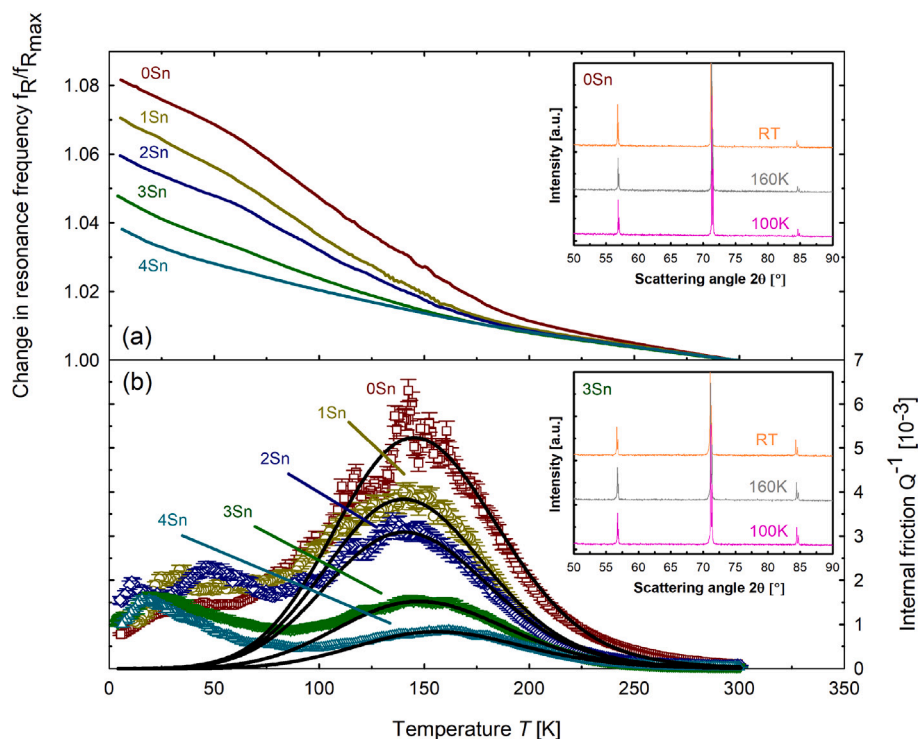
**Fig. 5.** Effect of Sn addition (1 at.% yellow circle, 2 at.% blue diamond, 3 at.% green triangle down, 4 at.% cyan triangle down) on the (a) change in resonance frequency $f_R/f_{R_{max}}$ and (b) internal friction response $Q^{-1}$ of the Ti4Mo8Cr alloy (red rectangle) upon continuous cooling. Furthermore, the fit of the internal friction response $Q^{-1}$ derived using a modified Debeye-oscillator model (Eqs. (2)–(4)) is shown (black lines). The accuracy of the internal friction response was estimated from the decay of the acoustic resonance mode with 5 %. With increasing Sn-content, the change in resonance frequency flattens accompanied by a significantly decreasing internal friction response. The insets show the XRD patterns at room temperature (RT) and cryogenic temperatures for Ti4Mo8Cr and Ti4Mo8Cr3Sn. Both indicate that no $\omega_{ath}$-formation occurred possibly responsible for the change in internal friction response. (For interpretation of the references to colour in this figure legend, the reader is referred to the web version of this article.)
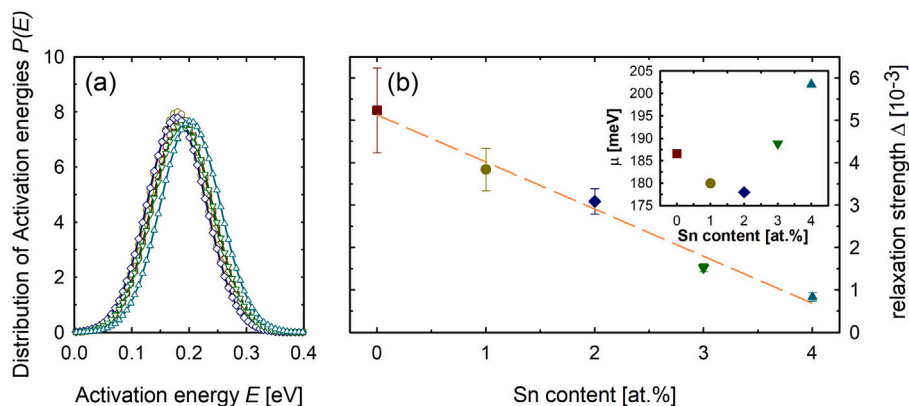


**Fig. 6.** Effect of Sn addition (1 at.% yellow circle, 2 at.% blue diamond, 3 at.% green triangle down, 4 at.% cyan triangle down) on the elementary process of $\omega$-formation derived using a modified Debeye-oscillator model (Eqs. (2)–(4)). (a) Distribution of activation energies $P(E)$ for the elementary process and (b) relaxation strength $\Delta$ dependent on Sn-content (inset shows the mean activation energy $\mu$). The modified Debeye-oscillator model revealed that the activation energy of the elementary process of $\omega$-formation seems to not be influenced by the addition of Sn. The relaxation strength linearly decreases with increasing Sn-content indicating a diminishing of local collapse regions where $\omega$-nuclei might form.

diffusion of solute-atoms was observed by Bó et al. [48] in Ti–Nb–Fe gum metals after the addition of 6 wt% Sn using energy dispersive X-ray spectroscopy (EDX) with negligible partitioning of Nb and Fe after isothermal ageing at 450 °C. Consequently, those local regions remain longer in the stable $\beta$-phase. With increasing Sn content, the tendency to form solute-cluster surrounding vacancies might even rise, more efficiently immobilising the vacancies as similarly found in $\alpha$-Zr. [49,50] Compared to Al-based alloys, which show only a very low solubility for Sn (several hundred ppm) within their matrix, the comparably high Sn content seems to inhibit or retard the release of the trapped vacancies towards higher temperatures as no decisively

accelerated $\omega$-phase formation is observed. Furthermore, the high Sn-solute content incorporated in the $\beta$-alloys might lead to stress fields which will impede the ordering of the linear defects needed for the $(111)_\beta$-plane collapse. We assume, that both mechanisms will contribute to the observed reduction of collapse regions whereby solute-vacancy complexes starve the diffusion of Cr to form local $\beta$-stabiliser-lean regions and the stress field induced by the solutes might interact with the linear defects necessary for the elementary process. Apart from this kinetic explanation, it is well known from literature that the transition from the $\beta$- to the $\omega$-phase is a martensitic-type transformation obeying the orientation relationship $(0001)_\omega \,||\, (111)_\beta$, $[11\bar{2}0]_\omega \,||\, [011]_\beta$ between the $\beta$- and $\omega$-lattices. [5,6,15,51] As shown by several

authors for eutectoid Ti-Fe alloys [52–54], tuning the stabiliser-content modifies the lattice misfit between the $\omega$-phase and the surrounding $\beta$-matrix, where the best coincidence and, therefore, highest volume fraction of retained $\omega$-phase after severe plastic deformation was found at $\approx 4$ wt% Fe. With further increasing the local stabiliser-content, the crystal structure of the $\omega$-phase increasingly distorts resembling more and more the ordinary bcc solid solution and the retained volume fraction of $\omega$-phase decreased decisively. [53–55] Similar to the Ti-Fe and Ti-V system, the degree of misfit is high in the Ti-Cr system. [6,31] Therefore, it might be evident that the addition of Sn influences the martensitic-type transformation by modifying the misfit between the $\omega$- and $\beta$-phase leading to the strongly suppressed formation of the $\omega$-phase. Based on this picture, we would expect a distinct increase of the mean activation energy in the internal friction response of the elementary formation process rather than a pronounced deceleration of the transformation kinetics as observed by Tane et al. [33] for Ti-V alloys with increasing $\beta$-stability. Therefore, we assume that such an effect plays only a minor role in the observed effect by Sn additions. However, for future research it might be valuable to evaluate if the observed suppression of the $\omega$-phase after thermal treatment persists under applied shear strain.

## 5. Conclusions

The objective of this study was to evaluate the effect of Sn addition on the $\omega_{iso}$-phase formation in prototypical metastable $\beta$-Ti alloys. The detrimental effect of $\omega_{iso}$-phase formation on the mechanical properties leads to the ultimate goal of appropriate alloy design in order to suppress the elementary formation process. Through the combination of high stability laser dilatometry with ex-situ XRD under isothermal conditions, we have found that the addition of Sn strongly decelerates or even suppresses the precipitation kinetics of $\omega_{iso}$-phase by more than one order of magnitude to prolonged ageing times. Furthermore, the onset of the $\omega \rightarrow \alpha$ transformation shifted to ageing temperature exceeding $370\,°C$. The elementary process of $\omega$-transformation seems to be not affected by the addition of Sn resulting in a nearly unchanged mean activation energy of $\sim 0.2\,eV$ for the local collapse of $[111]_\beta$-planes determined using a modified Debye-oscillator model. However, we have shown that the relaxation strength decreases linearly with increasing Sn content suggesting an active reduction of local collapse regions that might form stable $\omega$-nuclei. We suggest, that this reduction of local collapse regions and the associated decisive impact on formation kinetics is evoked by the effective trapping of vacancies by the introduced Sn-solutes thereby hampering the local decomposition in $\beta$-stabiliser-lean and -rich regions. Furthermore, stress fields induced by the Sn-solutes will impede the ordering of linear displacement defects necessary for the elementary process to take place.

Summarising, these results show that the addition of Sn effectively suppresses the $\omega_{iso}$-formation opening up possibilities for advanced alloy design and manufacturing routes. The addition of Sn facilitates the opportunity for tailorable $\omega$-phase formation kinetics. Furthermore, the results clearly show that the width of the time–temperature process window and the long-time ageing resistance of $\beta$-alloys can be significantly increased. As conventional manufacturing techniques of Ti-alloys are highly time, material and energy consuming, additive manufacturing techniques gained increasing attention. [56] Additive manufacturing processes such as selective laser melting (SLM) are able to produce complex shaped parts nearly without post-processing, which saves time and simplifies the manufacturing process. [56] However, these techniques face severe obstacles such as temperature gradients, which may result in the formation of metastable phases such as the investigated $\omega$-phase. [56–58] Therefore, with regards to additive manufacturing methods such as SLM, the prevention of $\omega$-phase formation during cyclic reheating, allows for the creation of ready-to-use parts exploiting the low elastic moduli of the $\beta$-phase. This can be especially useful for tailored biomedical implants adjusted to the patient needs.

## References

[1] R.A. Antunes, C.A.F. Salvador, M.C.L. Oliveira, Materials Selection of Optimized Titanium Alloys for Aircraft Applications, Mater. Res. 21 (2) (2018) http://dx.doi.org/10.1590/1980-5373-mr-2017-0979.

[2] C. Leyens, M. Peters, Titanium and Titanium Alloys: Fundamentals and Applications, first ed., Wiley-VCH, 2003.

[3] M. Geetha, A.K. Singh, R. Asokamani, A.K. Gogia, title=the ultimate choice for orthopaedic implants - A review biomaterials, Prog. Mater. Sci. 54 (3) (2009) 397–425, http://dx.doi.org/10.1016/j.pmatsci.2008.06.004.

[4] M. Niinomi, C.J. Boehlert, Titanium alloys for biomedical applications, in: Springer Series in Biomaterials Science and Engineering, Springer Berlin Heidelberg, 2015, pp. 179–213, http://dx.doi.org/10.1007/978-3-662-46836-4_8.

[5] S.K. Sikka, Y.K. Vohra, R. Chidambaram, Omega phase in materials, Prog. Mater. Sci. 27 (1) (1982) 245–310, http://dx.doi.org/10.1016/0079-6425(82)90002-0.

[6] B.S. Hickman, The formation of omega phase in titanium and zirconium alloys: A Review, J. Mater. Sci. 4 (6) (1969) 554–563, http://dx.doi.org/10.1007/bf00550217.

[7] W. Petry, A. Heiming, J. Trampenau, M. Alba, G. Vogl, Strong phonon softening in the BCC phase of titanium, Phys. B: Condens. Matter 156–157 (1989) 56–58, http://dx.doi.org/10.1016/0921-4526(89)90585-1.

[8] D.D. Fontaine, N.E. Paton, J.C. Williams, The omega phase transformation in titanium alloys as an example of displacement controlled reactions, Acta Metall. 19 (11) (1971) 1153–1162, http://dx.doi.org/10.1016/0001-6160(71)90047-2.

[9] W. Petry, A. Heiming, J. Trampenau, M. Alba, C. Herzig, H.R. Schober, G. Vogl, Phonon dispersion of the bcc phase of group-IV metals. I. bcc titanium, Phys. Rev. B 43 (13) (1991) 10933–10947, http://dx.doi.org/10.1103/physrevb.43.10933.

[10] D.D. Fontaine, O. Buck, A Monte Carlo simulation of the omega phase transformation, Phil. Mag. 27 (4) (1973) 967–983, http://dx.doi.org/10.1080/14786437308227573.

[11] J.C. Williams, D. Fontaine, N.E. Paton, The $\omega$-phase as an example of an unusual shear transformation, Metall. Trans. 4 (12) (1973) 2701–2708, http://dx.doi.org/10.1007/bf02644570.

[12] J.M. Sanchez, D.D. Fontaine, The omega phase transformation, J. Phys. Colloq. 38 (C7) (1977) 444–452, http://dx.doi.org/10.1051/jphyscol:1977788.

[13] N.L. Okamoto, S. Kasatani, M. Luckabauer, M. Tane, T. Ichitsubo, Effects of solute oxygen on kinetics of diffusionless isothermal $\omega$ transformation in $\beta$-titanium alloys, Scr. Mater. 188 (2020) 88–91, http://dx.doi.org/10.1016/j.scriptamat.2020.07.005.

[14] R.J. Enzinger, M. Luckabauer, N.L. Okamoto, T. Ichitsubo, W. Sprengel, R. Würschum, Influence of Oxygen on the Kinetics of Omega and Alpha Phase Formation in Beta Ti-V, Metall. Mater. Trans. A 54 (2) (2022) 473–486, http://dx.doi.org/10.1007/s11661-022-06881-1.

[15] J. Ballor, T. Li, F. Prima, C.J. Boehlert, A. Devaraj, A review of the metastable omega phase in beta titanium alloys: the phase transformation mechanisms and its effect on mechanical properties, Int. Mater. Rev. 68 (1) (2022) 26–45, http://dx.doi.org/10.1080/09506608.2022.2036401.

[16] M.A.-H. Gepreel, M. Niinomi, Biocompatibility of Ti-alloys for long-term implantation, J. Mech. Behav. Biomed. Mater. 20 (2013) 407–415, http://dx.doi.org/10.1016/j.jmbbm.2012.11.014.

[17] J.C. Williams, B.S. Hickman, D.H. Leslie, The effect of ternary additions on the decompositon of metastable beta-phase titanium alloys, Metall. Trans. 2 (2) (1971) 477–484, http://dx.doi.org/10.1007/bf02663337.

[18] D.C. Zhang, S. Yang, M. Wei, Y.F. Mao, C.G. Tan, J.G. Lin, Effect of Sn addition on the microstructure and superelasticity in Ti-Nb-Mo-Sn Alloys, J. Mech. Behav. Biomed. Mater. 13 (2012) 156–165, http://dx.doi.org/10.1016/j.jmbbm.2012.04.017.

[19] P.E.L. Moraes, R.J. C., A. Lopes, R. Robin, E.S.N. Caram, Effects of Sn addition on the microstructure, mechanical properties and corrosion behavior of Ti-Nb-Sn alloys, Mater. Charact. 96 (2014) 273–281, http://dx.doi.org/10.1016/j.matchar.2014.08.014.

[20] T.S. Luhman, R. Taggart, D.H. Polonis, A resistance anomaly in beta stabilized Ti-Cr alloys, Scr. Metall. 2 (3) (1968) 169–172, http://dx.doi.org/10.1016/0036-9748(68)90219-6.

[21] M. Luckabauer, W. Sprengel, R. Würschum, A high-stability non-contact dilatometer for low-amplitude temperature-modulated measurements, Rev. Sci. Instrum. 87 (7) (2016) 075116, http://dx.doi.org/10.1063/1.4959200.

[22] H. Ogi, H. Ledbetter, S. Kim, M. Hirao, Contactless mode-selective resonance ultrasound spectroscopy: Electromagnetic acoustic resonance, J. Acoust. Soc. Am. 106 (2) (1999) 660–665, http://dx.doi.org/10.1121/1.427607.

[23] M. Hirao, H. Ogi, Free-decay measurement for attenuation and internal friction, in: EMATs for Science and Industry, Springer US, 2003, pp. 93–102, http://dx.doi.org/10.1007/978-1-4757-3743-1_6.

[24] M. Bönisch, A. Panigrahi, M. Stoica, M. Calin, E. Ahrens, M. Zehetbauer, W. Skrotzki, J. Eckert, Giant thermal expansion and α-precipitation pathways in Ti-alloys, Nature Commun. 8 (1) (2017) http://dx.doi.org/10.1038/s41467-017-01578-1.

[25] Q.-M. Hu, S.-J. Li, Y.-L. Hao, R. Yang, B. Johansson, L. Vitos, Phase stability and elastic modulus of Ti alloys containing Nb, Zr, and/or Sn from first-principles calculations, Appl. Phys. Lett. 93 (12) (2008) 121902, http://dx.doi.org/10.1063/1.2988270.

[26] J.L. Murray, The Cr-Ti (Chromium-Titanium) system, Bull. Alloy Phase Diagr. 2 (2) (1981) 174–181, http://dx.doi.org/10.1007/bf02881474.

[27] B.A. Borok, E.K. Novikova, L.S. Golubeva, R.P. Shchegoleva, N.A. Ruchéva, Dilatometric investigation of binary alloys of titanium, Met. Sci. Heat Treat. 5 (2) (1963) 94–98, http://dx.doi.org/10.1007/bf00650697.

[28] V.N. Moiseev, The properties and heat treatment of Ti-Cr and Ti-Cr-Al alloys, Met. Sci. Heat Treat. 5 (2) (1963) 87–94, http://dx.doi.org/10.1007/bf00650696.

[29] R.H. Ericksen, R. Taggart, D.H. Polonis, The martensite transformation in Ti-Cr binary alloys, Acta Metall. 17 (5) (1969) 553–564, http://dx.doi.org/10.1016/0001-6160(69)90114-x.

[30] T.S. Luhman, R. Taggart, D.H. Polonis, Correlation of superconducting properties with the beta to omega phase transformation in Ti-Cr alloys, Scr. Metall. 3 (11) (1969) 777–782, http://dx.doi.org/10.1016/0036-9748(69)90178-1.

[31] V. Chandrasekaran, R. Taggart, D. Polonis, An electron microscopy study of the aged omega phase in Ti-Cr alloys, Metallography 11 (2) (1978) 183–198, http://dx.doi.org/10.1016/0026-0800(78)90035-6.

[32] F. Sun, D. Laillé, T. Gloriant, Thermal analysis of the ω nanophase transformation from the metastable β Ti-12Mo alloy, J. Therm. Anal. Calorim. 101 (1) (2010) 81–88, http://dx.doi.org/10.1007/s10973-010-0713-0.

[33] M. Tane, H. Nishiyama, A. Umeda, N.L. Okamoto, K. Inoue, M. Luckabauer, Y. Nagai, T. Sekino, T. Nakano, T. Ichitsubo, Diffusionless isothermal omega transformation in titanium alloys driven by quenched-in compositional fluctuations, Phys. Rev. Mater. 3 (4) (2019) 043604, http://dx.doi.org/10.1103/physrevmaterials.3.043604.

[34] A.W. Sommer, S. Motokura, K. Ono, O. Buck, Relaxation processes in metastable beta titanium alloys, Acta Metall. 21 (4) (1973) 489–497, http://dx.doi.org/10.1016/0001-6160(73)90207-1.

[35] C.W. Nelson, D.F. Gibbons, R.F. Hehemann, Acoustic Relaxations in Zirconium-Niobium Alloys, J. Appl. Phys. 37 (13) (1966) 4677–4682, http://dx.doi.org/10.1063/1.1708116.

[36] A. Nowick, B. Berry, Anelastic Relaxation in Crystalline Solids, Elsevier, 1972, http://dx.doi.org/10.1016/b978-0-12-522650-9.x5001-0.

[37] T. Ozaki, H. Matsumoto, S. Watanabe, S. Hanada, Beta Ti Alloys with Low Young's Modulus, Mater. Trans. 45 (8) (2004) 2776–2779, http://dx.doi.org/10.2320/matertrans.45.2776.

[38] S. Hanada, H. Matsumoto, S. Watanabe, Mechanical compatibility of titanium implants in hard tissues, Int. Congr. Ser. 1284 (2005) 239–247, http://dx.doi.org/10.1016/j.ics.2005.06.084, interface Oral Health Science.

[39] S. Hanada, N. Masahashi, S. Semboshi, T.K. Jung, Low Young's modulus of cold groove-rolled β Ti-Nb-Sn alloys for orthopedic applications, Mater. Sci. Eng. A 802 (2021) 140645, http://dx.doi.org/10.1016/j.msea.2020.140645.

[40] H. Matsumoto, S. Watanabe, N. Masahashi, S. Hanada, Composition dependence of young's modulus in Ti-V, Ti-Nb, and Ti-V-Sn alloys, Metall. Mater. Trans. A 37 (2006) 3239–3249, http://dx.doi.org/10.1007/BF02586159.

[41] D. Choudhuri, Y. Zheng, T. Alam, R. Shi, M. Hendrickson, S. Banerjee, Y. Wang, S.G. Srinivasan, H. Fraser, R. Banerjee, Coupled experimental and computational investigation of omega phase evolution in a high misfit titanium-vanadium alloy, Acta Mater. 130 (2017) 215–228, http://dx.doi.org/10.1016/j.actamat.2017.03.047.

[42] Q.M. Hu, D.S. Xu, D. Li, First-principles investigations of the solute-vacancy interaction energy and its effect on the creep properties of α-titanium, Phil. Mag. A 81 (12) (2001) 2809–2821, http://dx.doi.org/10.1080/01418610108217166.

[43] L.-J. Zhang, Z.-Y. Chen, Q.-M. Hu, R. Yang, On the anbomal fast diffusion of solute atoms in α-Ti: A first-principles investigation, J. Alloys Compd. 740 (2018) 156–166, http://dx.doi.org/10.1016/j.jallcom.2017.12.359.

[44] C. Wolverton, Solute-vacancy binding in aluminum, Acta Mater. 55 (17) (2007) 5867–5872, http://dx.doi.org/10.1016/j.actamat.2007.06.039.

[45] M. Werinos, H. Antrekowitsch, T. Ebner, R. Prillhofer, W.A. Curtin, P.J. Uggowitzer, S. Pogatscher, Design strategy for controlled natural aging in Al-Mg-Si alloys, Acta Mater. 118 (2016) 296–305, http://dx.doi.org/10.1016/j.actamat.2016.07.048.

[46] S. Pogatscher, H. Antrekowitsch, M. Werinos, F. Moszner, S.S.A. Gerstl, M.F. Francis, W.A. Curtin, J.F. Löffler, P.J. Uggowitzer, Diffusion on Demand to Control Precipitation Aging: Application to Al-Mg-Si Alloys, Phys. Rev. Lett. 112 (22) (2014) 225701, http://dx.doi.org/10.1103/physrevlett.112.225701.

[47] J. Čížek, O. Melikhova, I. Procházka, J. Kuriplach, I. Stulíková, P. Vostrý, J. Faltus, Annealing process in quenched Al-Sn alloys: A positron annihilation study, Phys. Rev. B 71 (6) (2005) 064106, http://dx.doi.org/10.1103/physrevb.71.064106.

[48] M.R.D. Bó, C.A.F. Salvador, M.G. Mello, D.D. Lima, G.A. Faria, A.J. Ramirez, R. Caram, The effect of Zr and Sn additions on the microstructure of Ti-Nb-Fe gum metals with high elastic admissible strain, Mater. Des. 160 (2018) 1186–1195, http://dx.doi.org/10.1016/j.matdes.2018.10.040.

[49] G.M. Hood, R.J. Schultz, Defect recovery in electron-irradiated α-Zr single crystals: A positron annihilation study, J. Nucl. Mater. 151 (2) (1988) 172–180, http://dx.doi.org/10.1016/0022-3115(88)90069-4.

[50] G.M. Hood, Point defect diffusion in α-Zr, J. Nucl. Mater. 159 (1988) 149–175, http://dx.doi.org/10.1016/0022-3115(88)90091-8.

[51] A. Devaraj, S. Nag, R. Srinivasan, R. Williams, S. Banerjee, R. Banerjee, H. Fraser, Experimental evidence of concurrent compositional and structural instabilities leading to ω precipitation in titanium-molybdenum alloys, Acta Mater. 60 (2) (2012) 596–609, http://dx.doi.org/10.1016/j.actamat.2011.10.008.

[52] B.B. Straumal, A.R. Kilmametov, Y. Ivanisenko, A.S. Gornakova, A.A. Mazilkin, M.J. Kriegel, O.B. Fabrichnaya, B. Baretzky, H. Hahn, Phase Transformations in Ti-Fe Alloys Induced by High-Pressure Torsion, Adv. Eng. Mater. 17 (12) (2015) 1835–1841, http://dx.doi.org/10.1002/adem.201500143.

[53] A. Kilmametov, Y. Ivanisenko, A. Mazilkin, B. Straumal, A. Gornakova, O. Fabrichnaya, M. Kriegel, D. Rafaja, H. Hahn, The α-Ti → ω and β-Ti → ω phase transformations in Ti-Fe alloys under high-pressure torsion, Acta Mater. 144 (2018) 337–351, http://dx.doi.org/10.1016/j.actamat.2017.10.051.

[54] M.J. Kriegel, A. Kilmametov, V. Klemm, C. Schimpf, B.B. Straumal, A.S. Gornakova, Y. Ivanisenko, O. Fabrichnaya, H. Hahn, D. Rafaja, Thermal Stability of Athermal ω-Ti(Fe) Produced upon Quenching of β-Ti(Fe), Adv. Eng. Mater. 21 (1) (2019) 1800158, http://dx.doi.org/10.1002/adem.201800158.

[55] G.I. Nosova, N.B. D'yakonova, I.V. Lyasotskii, Metastable phases of electron type in titanium alloys with 3d-metals, Met. Sci. Heat Treat. 48 (9) (2006) 427–432, http://dx.doi.org/10.1007/s11041-006-0111-1.

[56] L.-C. Zhang, H. Attar, M. Calin, J. Eckert, Review on manufacture by selective laser melting and properties of titanium based materials for biomedical applications, Mater. Technol. 31 (2) (2016) 66–76, http://dx.doi.org/10.1179/1753555715Y.0000000076.

[57] J. Chen, X. Liao, J. Shu, L. Zhou, C. Li, Y. Ren, Y. Niu, Microstructure tailoring of Ti-15Mo alloy fabricated by selective laser melting with high strength and ductility, Mater. Sci. Eng. A 826 (2021) 141962, http://dx.doi.org/10.1016/j.msea.2021.141962.

[58] T. Zhang, C.-T. Liu, Design of titanium alloys by additive manufacturing: A critical review, Adv. Powder Mater. 1 (1) (2022) 100014, http://dx.doi.org/10.1016/j.apmate.2021.11.001.